

VIKSER: Visual Knowledge-Driven Self-Reinforcing Reasoning Framework

Chao Wang, Chunbai Zhang, Yongxiao Tian, Yang Zhou, and Yan Peng

Abstract—Visual reasoning refers to the task of solving questions about visual information. Current visual reasoning methods typically employ pre-trained vision-language model (VLM) strategies or deep neural network approaches. However, existing efforts are constrained by limited reasoning interpretability, while hindering by the phenomenon of underspecification in the question text. Additionally, the absence of fine-grained visual knowledge limits the precise understanding of subject behavior in visual reasoning tasks. To address these issues, we propose VIKSER (Visual Knowledge-Driven Self-Reinforcing Reasoning Framework). Specifically, VIKSER, trained using knowledge distilled from large language models, extracts fine-grained visual knowledge with the assistance of visual relationship detection techniques. Subsequently, VIKSER utilizes fine-grained visual knowledge to paraphrase the question with underspecification. Additionally, we design a novel prompting method called Chain-of-Evidence (CoE), which leverages the power of “evidence for reasoning” to endow VIKSER with interpretable reasoning capabilities. Meanwhile, the integration of self-reflection technology empowers VIKSER with the ability to learn and improve from its mistakes. Experiments conducted on widely used datasets demonstrate that VIKSER achieves new state-of-the-art (SOTA) results in relevant tasks. Moreover, VIKSER achieves performance on par with leading proprietary models, such as the latest ChatGPT-5.

Index Terms—Chain-of-Evidence, Self-Reflection, Visual Knowledge, Visual Language Model, Visual Reasoning.

I. INTRODUCTION

Endowing machines with robust logical reasoning capabilities has been a long-standing goal of vision-language models (VLMs) [1]–[3]. A critical step toward realizing the goal lies in enhancing the model’s visual reasoning capabilities [4], [5]. Visual reasoning involves solving questions about visual information [6], [7], a task that necessitates precise alignment between visual and textual features, along with advanced logical reasoning skills [8]–[10]. Figure 1 illustrates a typical example of visual reasoning, where an agent must accurately align the image with the question and infer the intent through multiple steps of logical reasoning. The notable features of visual reasoning not only drive advancements in cross-modal learning [11], [12] but also contribute to enhancing machines’ logical reasoning abilities [9], [13], underscoring its substantial research significance.

Existing visual reasoning methods typically employ pre-trained VLM strategies or deep neural network frameworks [1], [11], [14]. However, the reasoning capabilities of current efforts still exhibit limited interpretability (i.e., **Issue 1**).

Chao Wang, Chunbai Zhang, Yongxiao Tian, and Yan Peng are with the School of Future Technology, Shanghai University, Shanghai, 200444, China.

Yang Zhou is with the School of Mechatronic Engineering and Automation, Shanghai University, Shanghai 200444, China.

Chao Wang is the corresponding author (e-mail: cwang@shu.edu.cn).

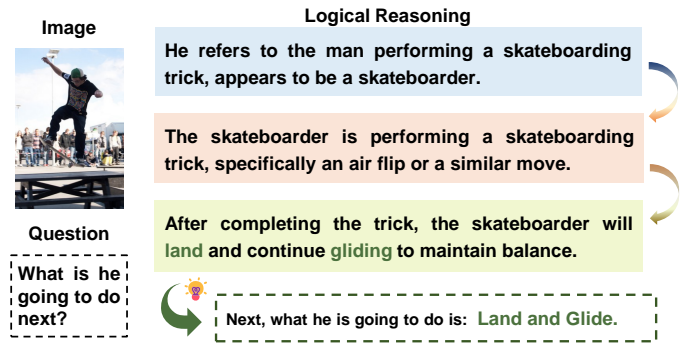


Fig. 1: A typical example of visual reasoning. This task requires an agent to accurately align the image with the question and infer the intent through multi-step logical reasoning.

Additionally, *underspecification* is a common phenomenon in visual reasoning tasks [9], [15], where a ambiguous description of the subject in the question text can hinder the alignment between textual and visual features, *leading to multiple incorrect visual interpretations and undermining reasoning reliability* (i.e., **Issue 2**). As shown in Figure 1, the subject “he” in the question is ambiguously described, which may be confused with other individuals in the image, presenting a risk of incorrect reasoning. On the other hand, visual knowledge extraction (VKE) techniques, which provide enriched visual information, have the potential to significantly assist in addressing visual reasoning tasks [16], [17]. However, *existing VKE methods are insufficient in extracting latent and fine-grained visual knowledge* (i.e., **Issue 3**). The issue limits the accurate understanding of subject behavior in complex questions, thereby hindering the interpretability and precision required for visual reasoning tasks.

To address these issues, we design VIKSER (Visual Knowledge-Driven Self-Reinforcing Reasoning Framework). The core components of VIKSER are the fine-grained visual knowledge extraction (F-VKE) module and the self-reinforcing reasoning (S-RR) module. For **Issue 1**, we deploy the S-RR module, which offers enhanced interpretability in reasoning and integrates self-reinforcement capabilities. Specifically, the module integrates a novel prompting technique, Chain-of-Evidence (CoE), which we propose to enhance interpretability by facilitating step-by-step reasoning grounded in factual evidence. Meanwhile, a self-reflection mechanism, which utilizes insights from past failures to refine future reasoning, is introduced to facilitate adaptive reinforcement. Additionally, intending to address **Issue 2**, a specification paraphrase method is explored for the S-RR module. Concretely, we collect object-level information from fine-grained visual knowledge to refine

ambiguous descriptions of the subject in question, thereby improving the question's clarity and completeness.

To address **Issue 3**, we deploy the F-VKE module to provide fine-grained visual knowledge to ViKSER. To be specific, the F-VKE module first detects the detailed visual relationships among key entities in an input image. Subsequently, we train the F-VKE module using knowledge distilled from large language models (LLMs) to uncover causal relationships between entities' behaviors and their inferred outcomes. For instance, as shown in Figure 3, LLMs can infer that a man depicted squatting on the right side of the train door may disembark at the next station. Following this, the trained F-VKE module leverages visual and causal relationships to generate fine-grained visual knowledge. A specific case that validates the fine-grained nature and richness of the visual knowledge generated by the F-VKE module is provided in Section IV-D. We conduct extensive experiments on diverse widely-recognized datasets to validate ViKSER's visual knowledge extraction and reasoning capabilities. The results demonstrate that ViKSER outperforms the latest research across all datasets, achieving new SOTA results. We summarize our **contributions** as follows:

- We propose ViKSER, a novel framework for visual reasoning tasks, which extracts fine-grained and enriched visual knowledge while performing highly interpretable and self-reinforcing reasoning.
- A specification paraphrase method is designed to help ViKSER mitigate underspecification, while a novel CoE prompting technique and a self-reflection mechanism are introduced to assist ViKSER in performing highly interpretable and self-reinforcing reasoning.
- Extensive experimental results demonstrate ViKSER's improvements over advanced baselines across diverse public datasets, achieving new SOTA results.

II. RELATED WORK

A. Visual Knowledge Extraction

Existing VKE methods either employ a holistic image captioning strategy or rely on fixed knowledge formats to extract visual information [2], [18]. Specifically, deep learning has played a crucial role in advancing image captioning approaches [19], [20]. With the development of VLMs, an increasing number of studies leverage pre-trained multimodal large language models (MLLMs) to understand both visual and textual information in a unified framework [21], [22]. On the other hand, the image captioning methods provide a broad understanding of the image content, yet they encounter challenges in conveying fine-grained details. In contrast, some studies utilize fixed knowledge graphs to map visual features to predefined semantic categories [17], [23], providing a structured form of visual knowledge [24], [25]. While these methods ensure consistency and interpretability, they fall short in providing enriched visual knowledge.

B. Language Model Reasoning

Recently, large VLMs have demonstrated remarkable success in reasoning and inference, particularly in facilitating few-shot [11], [26] and zero-shot [27], [28] learning. Notably,

through specialized training on diverse cross-modal benchmarks, VLMs have demonstrated advanced visual comprehension and reasoning abilities [1], [4], [29], significantly enhancing performance in visual reasoning tasks. Additionally, the potential of prompt-based reasoning [8], [9], [16] has been extensively explored to tackle diverse cross-modal visual reasoning tasks, including visual question answering (VQA) [4], [9], visual entailment (VE) [30], and visual commonsense reasoning (VCR) [8], [31]. By leveraging the substantial information embedded within VLMs, novel insights are generated to advance reasoning and interpretability research. In this paper, we aspire to employ fine-grained visual knowledge as factual grounding while implementing our interpretable, self-reinforcing reasoning paradigm to enhance performance on visual reasoning tasks.

III. METHOD

In this section, we provide detailed descriptions of ViKSER's F-VKE module (Section III-A) and S-RR module (Section III-B). Figure 2 illustrates a detailed framework of ViKSER. Next, we will provide a detailed introduction to the modules of ViKSER.

Specifically, the F-VKE module consists of two agents: the Visual Relationship Detector (*Ag-VRD*) and the Visual Knowledge enRicher (*Ag-VKR*), where *Ag-VKR* consists of a causal relationship analyzer G_a and an image caption generator G_c . Starting with the input image I and question Q , *Ag-VRD* first detects the visual relationships between key entities in I and integrates these relationships into a preliminary visual description D . Following this, G_a in *Ag-VKR* provides an analysis report A of the causal relationships between key entities' behaviors in D and their inferred outcomes. For instance, a description of a man squatting at the train door implicitly suggests that he may disembark at the next station. Finally, leveraging A , G_c in *Ag-VKR* enriches D into a more detailed and nuanced image caption C , offering fine-grained visual knowledge. On the other hand, the S-RR module is composed of the specification paraphraser (*Ag-SPR*) and the self-refining reasoner (*Ag-SR*). Specifically, *Ag-SPR* first collects visual information from C to refine ambiguous descriptions of the subject in Q , thereby forming the paraphrased question Q_r . Subsequently, *Ag-SR* employs CoE prompting to infer the predicted answer \tilde{a} based on Q_r , I , and C . When \tilde{a} exhibits positivity, it directly serves as the final answer a . Conversely, if \tilde{a} shows negativity, *Ag-SR* will use \tilde{a} and the reasoning trajectory t to perform self-reflection in search of a more valuable response. For the sake of readability, the key notations and their meanings used in this paper are systematically summarized in Table I.

A. F-VKE Module

Guided by the principles of multi-agent collaboration, the functionality of the F-VKE module in extracting fine-grained visual knowledge is distributed across two agents: the Visual Relationship Detector *Ag-VRD* and the Visual Knowledge enRicher *Ag-VKR*. The architectural design of *Ag-VRD* and the *Ag-VKR* is elaborated as follows.

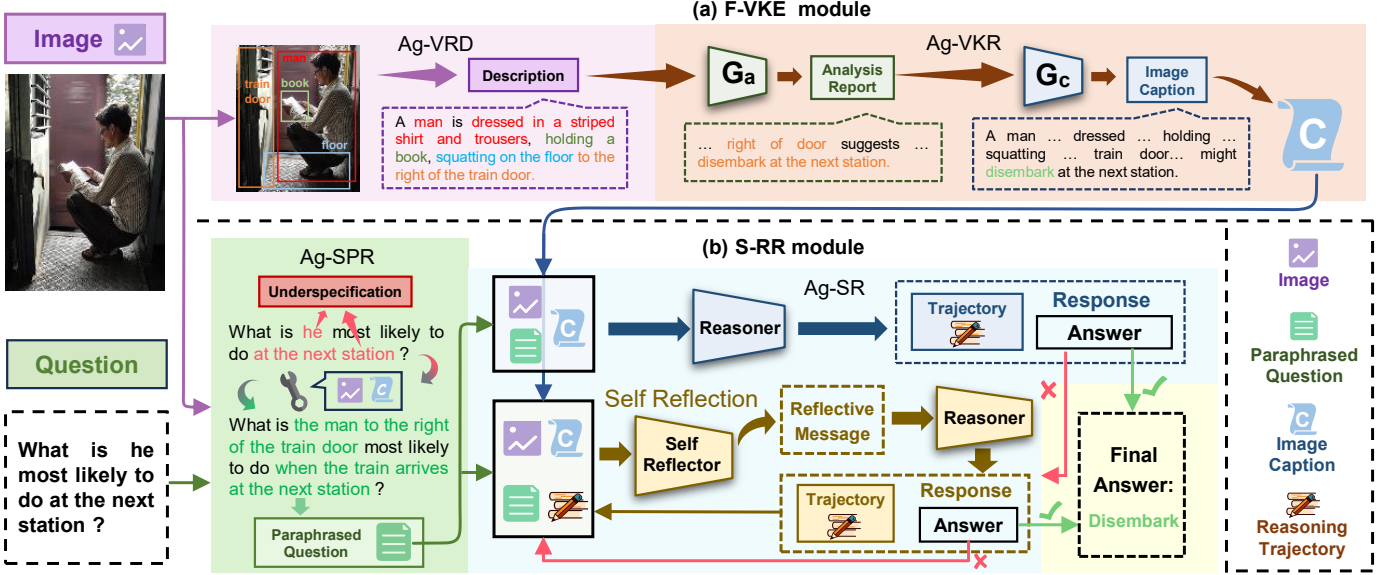


Fig. 2: **The framework of ViKSER.** Starting with the input image and question, ViKSER first extracts the relationships between key entities in the image and analyzes these relationships to form a detailed image caption. Then, ViKSER uses the image caption to paraphrase the question, refining the ambiguous descriptions in the question. Finally, ViKSER infers a predicted answer based on the paraphrased question, the image, and its caption. The predicted answer is taken as the final answer if it sufficiently addresses the question. Otherwise, ViKSER performs self-reflection based on the reasoning trajectory, the paraphrased question, the image, and its caption to seek a new response.

TABLE I: Comprehensive overview of the key notations and their meanings used in this paper.

Notation	Meaning
I	The input image
Q	The original question
E_K	The key entity
r	The visual relationship between E_K
R_K	The key visual relationship
D	The preliminary visual description
C	The detailed image caption
A	The analysis report about causal relationships between key entities' behaviors and their inferred outcomes
A_p	The pseudo-ground-truth causal relationship analysis report used in the knowledge distillation process
C_p	The pseudo-ground-truth image caption used in the knowledge distillation process
G_a	The causal relationship analyzer
G_c	The image caption generator
Q_r	The paraphrased question
\tilde{a}	The predicted answer to the question
a	The final answer to the question
t	The reasoning trajectory
S_{ref}	The discrete binary reward score assigned to \tilde{a}
V_{ref}	The verbal reflective message generated by the self-reflection mechanism

a) **Visual Relationship Detector:** Accurate detection of entities in images and their relationships form the foundation for effective VKE techniques. With the aim of endowing the F-VKE module with efficient visual relationship detection capabilities, we design the *Ag-VRD* based on existing VRD methods. Concretely, given an input image I , the *Ag-VRD* is prompted to extract all entities within the image. Each entity is then assigned a validity score S_e , reflecting its relevance in

understanding the image's content. Notably, when the entity's score exceeds a predefined threshold θ_e , it is classified as a key entity E_K . Following this, with the aid of CoVLM [24], we extract all relevant visual relationships of E_K . CoVLM is an exceptional VRD method that facilitates the collaboration between visual detection networks and LLMs, utilizing specially designed communication tokens. The advantage of CoVLM lies in its ability to precisely identify the target entity E_T corresponding to a given relationship based on the input entity E_I , by leveraging the specially crafted communication tokens. However, due to the fixed structure of its communication tokens, CoVLM is limited in offering fine-grained visual knowledge. Therefore, we utilize CoVLM primarily for refining the detected visual relationships.

To be specific, we first employ the detection network of CoVLM to identify the regions of interest corresponding to each E_K in I . Based on these regions and their associated entities, the *Ag-VRD* is then prompted to detect all potential relationships associated with E_K . Subsequently, we employ CoVLM to detect the relevant entities corresponding to these potential relationships. These potential relationships are then merged with their associated entities to form the visual relationship r . Following this, the *Ag-VRD* is employed to assess a relationship validity score S_r for each r based on its effectiveness in contributing to the understanding of I . To determine which visual relationships associated with the key entities are truly effective in capturing the semantics of the input image, we propose a joint entity-relation joint validity evaluation algorithm to compute the entity-relation joint validity score S_r^e :

$$S_r^e = S_e \cdot \omega_r \cdot S_r, \omega_r = 1 + \gamma(\alpha - N_r^e), \quad (1)$$

where S_e denotes the entity validity score and S_r denotes the relationship validity score. ω_r represents the weight associated with the current visual relationship r . N_r^e denotes the number of r held by the key entity E_K . γ and α are hyperparameters, where γ controls the influence of the number of visual relationships on the weight, constrained within the range (0.05, 0.2). And α limits the number of visual relationships. For example, as N_r^e increases, ω_r decreases to amplify the constraint of S_r^e on the visual relationship. Conversely, ω_r increases when the number of relationships is smaller. Additionally, in case S_r^e exceeds a threshold θ_r^e , the corresponding visual relationship under the current key entity is labeled as a key visual relationship R_K . After identifying E_K and R_K , we generate the preliminary image description D by progressively aligning each E_K with its corresponding key visual relationship R_K .

b) **Visual Knowledge Enricher:** Existing VRD methods primarily focus on detecting surface-level, concept-based relational information within an image [24], [32]. This nature makes it challenging for current VRD methods to conduct in-depth, object-level analysis of the image content. However, such analyses are essential for a comprehensive understanding of the image. For this reason, we further deploy Ag-VKR, which consists of a causal relationship analyzer G_a and an image caption generator G_c , to enhance the depth of knowledge in image analysis. Specifically, G_a first interprets the preliminary image description D concerning the input image I . Next, G_a derives an analysis report A that uncovers the causal relationships between the behaviors of key entities in D and their inferred outcomes. Subsequently, G_c enriches D by incorporating the visual knowledge from I and A , resulting in a detailed image caption C for I .

Causal relationship analysis reporting and detailed image captioning typically require training with ground-truth data, which is often absent in existing datasets. To address this, we propose leveraging the extensive knowledge reservoir inherent in LLMs (e.g., ChatGPT-4o [33]) to generate causal relationship analysis reports and detailed image captions as pseudo-ground-truth data to train G_a and G_c . Specifically, we extract pseudo-ground-truth causal relationship analysis report A_p from LLM with a task-specific set of few-shot demonstrations as follows:

$$KA_p = \{A_p \mid A_p \sim P_{LLM}(I, D)\}, \quad (2)$$

where I denotes the input image, D represents the ground-truth preliminary image description of I , and P_{LLM} denotes the LLM operating in an autoregressive manner. A_p represents the pseudo-ground-truth causal relationship analysis report sampled from P_{LLM} , and KA_p represents the set of all A_p . Notably, KA_p may be noisy and erroneous, which could adversely affect the subsequent detailed image captioning process. To address this, we apply a post-processing mechanism to filter KA_p into KA'_p . Specifically, for each A_p in KA_p , we use a pre-trained MLLM (e.g., ChatGPT-4o; denoted as F) to assess its validity score S_{A_p} based on whether A_p correctly uncovers the causal relationship. In case S_{A_p} exceeds a predetermined threshold τ , the corresponding A_p is retained. The process of collecting

KA'_p is formalized as follows:

$$KA'_p = \{A_p \mid S_{A_p} > \tau\}, S_{A_p} = F(A_p, (I, D)), \quad (3)$$

where A_p denotes the pseudo-ground-truth causal relationship analysis report. I denotes the input image, D represents the ground-truth preliminary image description of I . τ denotes the predetermined threshold. F denotes the pre-trained MLLM. With KA'_p serving as pseudo-ground-truth data, we are able to train G_a with the distillation loss L_{G_a} , as formalized below:

$$L_{G_a} = - \sum_{t=1}^T \log [P_{G_a}(A'_{p,t} \mid A'_{p,t-1}, (I, D))], \quad (4)$$

where $A'_p \in KA'_p$, and $T = |A'_p|$. Figure 3 shows how we utilize knowledge distillation from the LLM to train G_a . Specifically, for the Image and Description, a post-processing mechanism employs F to determine whether S_{A_p} is passing, thereby filtering out the noise from the LLM-generated A_p to obtain A'_p . Following this, A'_p is used to train G_a via L_{G_a} , in order to generate A .

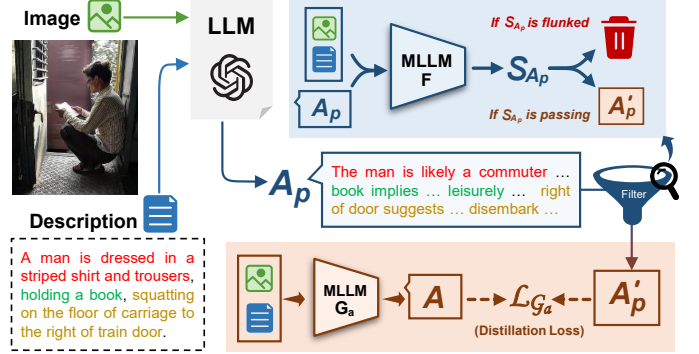


Fig. 3: Process of utilizing knowledge distillation from LLM to train G_a to generate A .

Similarly, we employ the same knowledge distillation approach to train G_c . Concretely, we utilize KA'_p as input to help G_c enrich the preliminary image description D , thereby generating pseudo-ground-truth image captions KC'_p . Subsequently, we train the image caption generator G_c with the distillation loss L_{G_c} described below:

$$L_{G_c} = - \sum_{t=1}^T \log [P_{G_c}(C'_{p,t} \mid C'_{p,t-1}, (I, D, A'_p))], \quad (5)$$

where $C'_p \in KC'_p$, $A'_p \in KA'_p$, and $T = |C'_p|$. More details are discussed in Appendix A and B0b. In summary, the trained causal relationship analyzer G_a and image caption generator G_c operate collaboratively to fulfill the functionality of Ag-VKR. Specifically, given an input image I and the preliminary image description D , G_a and G_c generate a detailed image caption C for I .

B. S-RR Module

We leverage the detailed visual knowledge in the image caption C , which is generated by the F-VKE module, to enhance the performance of ViKSER in visual reasoning tasks, such as VQA and VE. To achieve this, we propose an S-RR

module, consisting of a specification paraphraser *Ag-SPR* and a self-refining reasoner *Ag-SR*, to endow VIKSER with advanced reasoning capabilities. Specifically, starting with an image and a question, *Ag-SPR* extracts and analyzes the fine-grained visual knowledge in C , to refine ambiguous descriptions in the question and paraphrase it. Subsequently, *Ag-SR* resolves the paraphrased question by leveraging the input image and the detailed image caption through a self-reinforcing reasoning paradigm. It is important to emphasize that we aim to develop a reasoning approach characterized by high generalizability and a gradient-free, in light of the diversity of visual reasoning tasks. For this reason, we propose employing a flexible and plug-and-play reasoning prompt paradigm to prompt pre-trained visual language models (PVLMs) to perform the functions of *Ag-SPR* and *Ag-SR*. Detailed prompts are discussed in Appendix C. The architectural design of *Ag-SPR* and the *Ag-SR* is elaborated as follows.

a) Specification Paraphraser: Starting with the input image I , the original question Q , and the detailed image caption C generated by the F-VKE module, *Ag-SPR* leverages the detailed visual information in C to paraphrase Q , thereby refining any ambiguous descriptions within Q . We employ a PVLM as the core of *Ag-SPR* to facilitate this process. Specifically, we prompt the PVLM in *Ag-SPR* to first identify the main subject in Q , and then query the detailed image caption C for relevant textual information. Meanwhile, the PVLM is prompted to extract the interaction between the main subject and the image scene from C , providing a complementary description of the main subject's context. Subsequently, the above textual information is paraphrased in natural language and integrated into Q to form the paraphrased question Q_r . The underlying logic of this process is that the entities mentioned in Q intuitively provide key information relevant to the expected answer intuitively. For this reason, providing more detailed descriptions of the subject aids the S-RR module in resolving the visual reasoning task.

b) Self-Refining Reasoner: As a key component of the S-RR module, the cognitive and reasoning capabilities of *Ag-SR* significantly influence the overall problem-solving performance of the system. To enhance *Ag-SR*'s capabilities, we introduce a prompting technique called CoE, which guides *Ag-SR* to reason incrementally and provide highly interpretable steps toward the expected answer of Q_r . Furthermore, we present a self-reflection mechanism that allows *Ag-SR* to perform self-correction, thereby improving its robustness in reasoning. Detailed descriptions are as follows.

Highly Interpretable Reasoning: We prompt a PVLM to serve as the core of *Ag-SR*. Given that conventional reasoning prompts, such as “think step-by-step” [34], often induce hallucinations due to insufficiently grounded rationale, we propose CoE, a tailored prompting technique, to enhance the PVLM's reasoning ability. Concretely, the PVLM first analyzes fine-grained visual knowledge provided by the F-VKE module, extracting factual information to serve as evidence for reasoning. Subsequently, CoE guides the PVLM through a structured, step-by-step reasoning process based on the extracted evidence, ultimately generating a predicted answer \tilde{a} . This reasoning framework enables CoE to enhance interpretability while im-

proving reasoning accuracy. Further details on CoE prompting are provided in Appendix C0b. Additionally, we validate the effectiveness of the CoE prompting method in Section IV-C.

Self-Reflection-Based Reinforcement Mechanism: Existing research has shown that even highly intelligent agents are susceptible to generating low-quality answers, which significantly diminishes the accuracy of their reasoning and decision-making processes. To address this, we propose a self-reflection mechanism that builds upon the method proposed by Shinn et al [35]. The mechanism enables *Ag-SR* to manage instances of low-quality answers by leveraging past experiences, thereby reducing the likelihood of similar errors occurring in the future. Specifically, after deriving \tilde{a} , *Ag-SR* utilizes an exact matching mechanism to map complex natural language information in \tilde{a} to a two-dimensional discrete binary reward score S_{ref} . If S_{ref} is positive, the predicted answer \tilde{a} is directly used as the final answer a . In contrast, when S_{ref} is represented as negative, *Ag-SR* is prompted to analyze Q_r and a reasoning trajectory t from the previous trial. Subsequently, *Ag-SR* reflects on the cause of failure and generates a detailed verbal reflection, denoted as V_{ref} . Following this, V_{ref} serves as experiential knowledge to guide *Ag-SR* in generating a more accurate answer in subsequent trials. It is important to note that, compared to the reward score S_{ref} , V_{ref} encompasses more comprehensive experiential information. For instance, while S_{ref} merely indicates success or failure, V_{ref} provides insight into which aspects of the previous reasoning trajectory were incorrectly applied, resulting in previous failure. Furthermore, V_{ref} can provide guidance on how to avoid similar mistakes in future trials. Further details are discussed in Appendix B0a.

IV. EXPERIMENTS

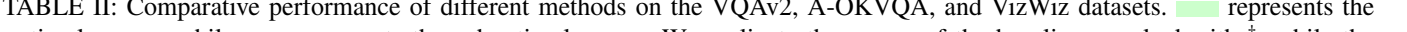
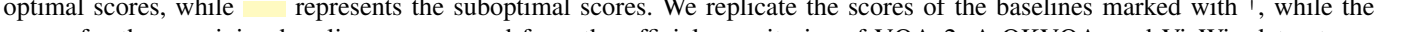
In this section, we conduct extensive experiments on publicly available datasets to evaluate VIKSER's performance on visual reasoning tasks.

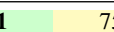
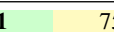
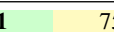
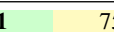
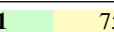
A. Experimental Setup

Datasets: To evaluate the reasoning abilities of VIKSER, we utilize widely-used datasets for visual reasoning tasks, including VQAv2 [36], A-OKVQA [37], VizWiz [38], e-SNLI-VE [30], COLA [5], and CREPE [39].

Baselines: We compare VIKSER with 22 competitive baselines, including SMoLA-PaLI-X [4], LLaVa-1.5-7B [2], Qwen-2.5 [40], ChatGPT-4o-mini [41], ChatGPT-4o [42], ChatGPT-5 [43], REPARSE [9], CoVLM [24], Molmo-72B [11], PaLi-X [29], PaliGemma 2 [1], NLX-GPT [31], LOCVLM-L [44], HIMIX [45], CIBI [46], MAVL [47], DIETCOKE [48], Rapper [8], e-UG [30], OFX-X [49], MosaiCLIP [50], CLIP+MM-Pred [5], and CLIP+ Linear [5].

Evaluation Metrics: Based on previous work [5], [8], [9], [39], we evaluate accuracy across distinct question types: yes/no (Y/N), number (Num.), other (Ot.), direct answer (DA.), and multiple-choice (MC.), as well as the overall accuracy (Ov.). Notably, for the COLA, CREPE, and e-SNLI-VE datasets, we report Accuracy (Acc.) directly. Additionally, for CREPE, we further evaluate Recall@1 (R@1).

TABLE II: Comparative performance of different methods on the VQAv2, A-OKVQA, and VizWiz datasets.  represents the optimal scores, while  represents the suboptimal scores. We replicate the scores of the baselines marked with \dagger , while the scores for the remaining baselines are sourced from the official repositories of VQAv2, A-OKVQA, and VizWiz datasets, as well as the study conducted by Prasad et al. [9].

Methods	VQAv2				A-OKVQA		VizWiz Ov. (%)
	Ov. (%)	Y/N (%)	Num. (%)	Ot. (%)	MC. (%)	DA. (%)	
<i>General Methods</i>							
LLaVa-1.5-7B \dagger	74.04	86.84	52.94	57.89	62.56	77.38	57.07
REPARE+LLaVa-1.5	77.34	92.64	59.92	70.12	66.19	78.21	59.46
REPARE+BLIP-2	74.05	94.56	54.40	63.36	55.67	82.80	70.03
Molmo-72B	86.67	96.91	 78.49	79.63	82.20	74.95	-
ChatGPT-4o-mini \dagger	75.54	81.69	65.46	76.41	82.76	78.79	80.61
ChatGPT-4o \dagger	86.98	93.44	71.43	 85.94	90.79	89.79	79.87
ChatGPT-5 \dagger	 88.68	93.86	77.86	85.33	 91.86	 90.47	82.15
<i>VRD Methods</i>							
CoVLM \dagger	48.80	64.02	36.85	40.37	46.47	52.35	44.32
<i>Task-Specific Methods</i>							
MAVL	-	-	-	-	53.80	50.70	-
DIETCOKE	-	-	-	-	49.20	48.60	-
LocVLM-L	55.90	68.73	40.45	46.37	-	-	-
HiMix	80.20	89.72	61.37	73.48	-	-	-
CIBi	61.59	82.02	43.60	51.79	-	-	-
SMoLA-PaLI-X	85.00	-	-	-	84.1	70.55	72.00
PaLI-X	86.06	96.78	74.14	79.46	80.4	68.20	73.30
PaLI-Gemma 2	86.95	 97.19	77.77	80.13	83.7	71.30	78.10
ViKSER (ours)	 88.74	 98.31	75.51	 86.71	 92.51	88.53	 82.52

Implementation Details We prompt GPT-4o mini [41] as the LLM foundation for Ag-VRD of the F-VKE module in ViKSER. Additionally, we employ LLaVa-1.5-7B [2] as the PVLM foundation for the S-RR module of ViKSER. It is important to note that in Section III-A0b, the LLM used for knowledge distillation is ChatGPT-4o [33], while G_a and G_c are obtained through training LLaVa-1.5-7B. On the other hand, a summary of the experimental setup is provided, which includes the datasets, baseline methods, and evaluation metrics employed for performance assessment.

B. Main Results

We conduct extensive experiments to validate ViKSER’s visual reasoning capabilities, with the main experimental results summarized as follows.

ViKSER performs outstandingly in reasoning and answering visual questions. To validate the superiority of ViKSER’s visual reasoning capabilities, we compare its performance with ten competitive baselines on the VQAv2, A-OKVQA, and VizWiz datasets, as presented in Table II. To be specific, ViKSER achieves new SOTA results across all datasets, with the exception of the Num. metric on VQAv2 and the DA. metric on A-OKVQA. Notably, when LLaVa-1.5-7B is used as the PVLM foundation for the S-RR module, ViKSER significantly outperforms LLaVa-1.5-7B across all metrics. In particular, on the MC. metric of the A-OKVQA dataset, ViKSER achieves an almost 30% improvement over LLaVa-1.5-7B. Meanwhile, ViKSER, employing a gradient-free reasoning paradigm, continues to outperform task-specific methods pre-trained on the datasets. These substantial ad-

vantages demonstrate the superiority and generalizability of ViKSER’s reasoning paradigm. Moreover, ViKSER, with fewer parameters, outperforms baselines with more parameters, such as ChatGPT-4o and Molmo-72B, across all metrics except for Num. and DA. The advancements highlight ViKSER’s potential in visual reasoning tasks.

On the other hand, we analyze the reasons for ViKSER’s slight underperformance on the Num. metric of the VQAv2 dataset as follows: (1) ViKSER has fewer model parameters, larger models, such as Molmo-72B, benefit from a larger parameter size; (2) ViKSER prioritizes extracting information from key entities in the image, which may lead to a potential risk of overlooking a holistic analysis of the image. For these reasons, ViKSER performs slightly worse on visual reasoning tasks involving numerical questions compared to more powerful LLMs, such as Molmo-72B. Nonetheless, we believe there is still room for improvement in ViKSER’s numerical analysis performance. Additionally, although ViKSER achieves a marginally lower score than ChatGPT-4o and ChatGPT-5 on the DA. metric of A-OKVQA, the performance gap is negligible, with differences of only 1.26 and 1.94 points, respectively. These results indicate that ViKSER attains comparable performance to ChatGPT-4o in visual reasoning tasks, demonstrating its competitiveness as an effective model.

ViKSER performs excellently in reasoning and understanding visual information. To further evaluate the reasoning performance of ViKSER, we compare it with nine competitive baselines on the COLA, CREPE dataset, as shown in Table III. Specifically, ViKSER outperforms existing methods, achieving a new SOTA result. Notably, both the COLA and CREPE

datasets require a model to precisely match images with captions. Therefore, the success of ViKSER highlights its capacity to accurately interpret image content and effectively extract information from key entities, enabling it to perform visual reasoning tasks with high precision.

TABLE III: Comparative performance of different methods on the Cola and CREPE datasets. The baseline scores are sourced from related studies [5], [24].

METHODS	COLA	CREPE	
	ACC. (%)	ACC. (%)	R@1 (%)
MOSAICLIP	-	-	90.2
CLIP + MM-PRED	41.42	77.84	-
CLIP + LINEAR	30.47	87.35	-
CoVLM	44.29	-	-
ViKSER (OURS)	49.49	96.68	93.81

Additionally, as demonstrated in Figure 4, ViKSER performs outstandingly on the e-SNLI-VE dataset. Notably, ViKSER surpasses OFX-X by 8.72%, highlighting its effectiveness. The success of ViKSER underscores its ability to correctly infer the visual scene present in an image based on the visual information. We attribute this advantage to the seamless collaboration between the F-VKE and S-RR modules, as well as the flexible reasoning paradigm within the S-RR module. As discussed in Section III-B, the plug-and-play nature and gradient-free design of the reasoning paradigm in the S-RR module endow ViKSER with high generalization capabilities, enabling it to adapt to diverse visual reasoning tasks.

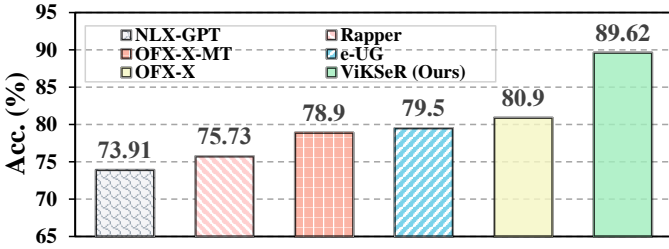


Fig. 4: Comparative performance of different methods on the e-SNLI-VE dataset. The baseline scores are sourced from the official repository of e-SNLI-VE and the seminal study conducted by Chang et al. [8].

ViKSER demonstrates remarkable adaptability across diverse LLMs. To further validate the adaptability of ViKSER, we conduct comparative experiments across three datasets: VQA-v2, A-OKVQA, and VizWiz. These experiments assess ViKSER when integrated with four distinct VLM and LLM backbones: LLaVa-1.5-7B, Qwen-2.5, ChatGPT-4o, and ChatGPT-5. Notably, to integrate ViKSER with various backbones, we utilize its original F-VKE module while adapting the S-RR module specifically for each VLM and LLM. The results, presented in Table IV, reveal that the integration of ViKSER yields significant performance improvements across all metrics and datasets for every backbone. This outcome demonstrates that ViKSER can be effectively transferred to diverse VLM

and LLM backends, delivering consistent gains and showcasing its strong generalization capabilities. Notably, the performance enhancement is more substantial for LLaVa-1.5-7B than for the ChatGPT series. The particularly remarkable gain on the O metric for VQA-v2 suggests that ViKSER, even when paired with a comparatively weaker backbone like LLaVa-1.5-7B, can achieve results competitive with those from powerful LLM backends, thereby validating its efficacy.

C. Ablation Studies

We conduct various ablation experiments to evaluate the performance of each component of ViKSER. Specifically, on the VQAv2 dataset, we systematically ablate the *Ag-SPR* and self-reflection mechanism in the *S-RR* module to assess their impact on the performance of ViKSER. As shown in Table V, on the VQAv2 dataset, ablating *Ag-SPR* individually results in the least impact on overall performance. In contrast, the simultaneous ablation of both *Ag-SPR* and the self-reflection mechanism leads to the most significant performance drop. To evaluate the performance of the *F-VKE* module, we conduct comparative experiments by ablating it and using LLaVA-1.5 and ChatGPT-4o as the LLM backbones for the *S-RR* module of ViKSER. As shown in the lower section of Table V, both ViKSER configurations exhibit significant performance drops without the *F-VKE* module. Notably, the LLaVA-1.5-based variant resulted in an approximately 15% performance decline. These results demonstrate that the fine-grained visual knowledge provided by the *F-VKE* module critically improves the model’s visual reasoning comprehension and processing.

Furthermore, to validate the efficacy of the *F-VKE* module, we conduct qualitative comparisons between ViKSER’s *F-VKE* module and three baseline models (LLaVA-1.5, Qwen-2.5, and GPT-4o-mini) on detailed image caption generation across four test cases. As shown in Figure 5 (upper panel), both LLaVA-1.5 and Qwen-2.5 generate hallucinated content in the first case, while GPT-4o-mini produces a more accurate scene description. Crucially, ViKSER’s caption demonstrates superior visual grounding through the *F-VKE* module, which not only correctly identifies image contents but also infers causal relationships embedded within the fine-grained details (e.g., “he just took a bite of the pastry” and “the scene occurs in cold weather conditions”). This pattern persists in the second case (Figure 5, lower panel), where LLaVA-1.5 and Qwen-2.5 again exhibit hallucination. Although GPT-4o-mini improves upon the baselines, it overemphasizes peripheral background elements. Fortunately, ViKSER’s *F-VKE* module consistently maintains its performance advantage, delivering precise descriptions while extracting implicit causal relationships (e.g., “the subject is likely preparing to disembark at the subsequent station”). Meanwhile, in two other cases illustrated in Figure 6, LLaVA-1.5 continues to exhibit severe hallucinations in its generated captions. While Qwen-2.5 and GPT-4o-mini provide relatively accurate scene descriptions, the latter disproportionately emphasizes irrelevant background details. Notably, the image captions generated by ViKSER’s *F-VKE* module, which incorporates fine-grained visual knowledge, not only accurately describe the scene but also reveal causal relationships. These

TABLE IV: Performance of ViKSER with different VLM and LLM backends (LLaVa-1.5-7B, Qwen-2.5, ChatGPT-4o, and ChatGPT-5) on three datasets (VQA-v2, A-OKVQA, and VizWIZ). "Base" denotes the original performance of each model, and "+ViKSER" denotes its performance after being enhanced by the ViKSER framework.

Datasets	Metrics	LLaVa-1.5-7B		Qwen-2.5		ChatGPT-4o		ChatGPT-5	
		Base	+ViKSER	Base	+ViKSER	Base	+ViKSER	Base	+ViKSER
VQA-v2	Ov. (%)	74.04	88.74	64.73	72.45	86.98	95.52	88.68	97.13
	YN (%)	86.84	98.31	71.25	87.50	93.44	98.98	93.86	98.76
	Num. (%)	52.94	75.51	45.38	68.50	71.43	85.57	77.86	87.89
	Ot. (%)	57.89	86.71	49.78	79.63	85.94	93.75	85.33	96.15
A-OKVQA	MC. (%)	62.56	92.51	56.55	81.35	90.79	96.83	91.86	97.26
	DA. (%)	77.38	88.53	68.93	79.35	89.79	95.27	90.47	95.87
VizWIZ	Ov. (%)	57.07	82.52	55.73	77.86	79.87	88.68	82.15	89.79

TABLE V: Ablation results of experiments conducted on the VQAv2 and Cola datasets. w/o PARAPHRASER denotes the ablation of Ag-SPR, and w/o REFLECTION denotes the ablation of the self-reflection mechanism.

METHODS	VQAv2
	OVERALL (%)
ViKSER (OURS)	88.74
w/o PARAPHRASER	81.68
w/o REFLECTION	77.86
w/o PARAPHRASER AND REFLECTION	74.04

findings suggest that the F-VKE module effectively learns causal relationship inference capabilities from LLMs through knowledge distillation, enabling it to consistently produce captions enriched with fine-grained visual knowledge.



Caption: Llava 1.5

The image features a young boy with blonde hair, wearing a brown shirt and holding a piece of food in his hand. He appears to be enjoying the treat, possibly a donut, as he looks at it. There are two other people in the background, one on the left side and the other on the right side of the image.

Caption: GPT-4o-mini

A young boy is focused on his treat, with powdered sugar on his mouth, suggesting he just took a bite of a dessert. He is wearing a brown shirt and has his eyes lowered. The background shows blurred figures and strollers, suggesting an outdoor event. The scene evokes a relaxed, joyful atmosphere ...

Caption: Qwen2.5

The image shows a young child with light blonde hair, wearing a brown jacket over a white shirt ... The child is focused on eating a small pastry or donut dusted with powdered sugar. The child's eyes are closed as they take a bite, and there is some powdered sugar on their lips and chin.

Caption: ViKSeR (Ours)

A young child with blonde hair, wearing a brown jacket ... holding a pastry covered in powdered sugar ... There is powdered sugar on the child's mouth, suggesting he just took a bite of the pastry ... The child appears curious and focused as he takes a bite of the pastry, likely exploring its taste ... The brown jacket worn by the child suggests that the scene is taking place in colder weather.



Caption: Llava 1.5

The painting depicts a man sitting on the floor of a train, reading a book ... He is surrounded by several chairs, some of which are very close to him ... The train appears to be a commuter train, as it is filled with chairs and people. The man is focused on his book, enjoying his journey...

Caption: Qwen2.5

The image shows a person sitting on the floor near an open door, reading a book or a document. The setting appears to be inside a train compartment, as indicated by the window frame visible in the background ... The lighting suggests it might be daytime, and the person seems focused on their reading material.

Caption: ViKSeR (Ours)

A train is traveling along the tracks. A man, dressed in a striped shirt and trousers, is squatting on the floor of the carriage on the right side of the train door, holding a book in his hand ... The man appears to be a commuter, using his time on the train to read ... The fact that he is squatting on the floor of the carriage on the right side of the train door indicates that he might disembark at the next station.

Fig. 5: Performance of ViKSER's F-VKE module and baselines in generating captions for two images.

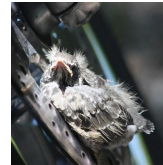


Caption: Llava 1.5

The image features a black and white cat sitting on a table in front of a television. The cat appears to be watching the TV screen, which displays a picture of another cat. The television is placed on the left side of the table, and the cat is positioned on the right side.

Caption: Qwen2.5

The image shows a domestic cat sitting in front of an LG television, seemingly captivated by the screen ... The TV displays another cat lying on a light-colored blanket, which appears to be part of a video or photograph ... The setting is indoors, with the television placed on a table covered with a lace tablecloth.

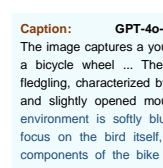


Caption: GPT-4o-mini

The image shows an inquisitive tabby cat with striking stripes is sitting in front of a television screen, engrossed in the image of another cat displayed on the screen ... The tabby cat, with its ears perked up and head slightly tilted, seems fascinated by the on-screen feline, adding a touch of humor and curiosity to the moment ...

Caption: ViKSeR (Ours)

The image shows a real tabby cat sits attentively on a table, facing towards a television screen that displays an image of another gray cat lounging comfortably on a bed, with a soft blanket underneath it ... The cat's positioning and focused gaze suggest that it is engaged in observing the cat on the screen, reflecting its natural curiosity and attentiveness to stimuli.

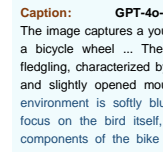


Caption: Llava 1.5

The image features a small bird perched on a bicycle seat, possibly a baby bird ... The bird is sitting on the seat, looking upwards, and appears to be curious about its surroundings. The bicycle is parked in a shaded area, providing a comfortable spot for the bird to rest...

Caption: Qwen2.5

The image shows a small, fluffy bird resting on what appears to be a metallic surface, possibly part of a bicycle wheel or a similar structure ... The bird has a soft, downy appearance with grayish-brown feathers that are not fully grown, suggesting it is a young or fledgling bird..



Caption: GPT-4o-mini

The image captures a young, fluffy bird resting on a bicycle wheel ... The bird appears to be a fledgling, characterized by its disheveled feathers and slightly opened mouth ... The surrounding environment is softly blurred out, indicating the focus on the bird itself, while hints of metallic components of the bike are visible, showcasing the stark contrast between nature and machinery.

Caption: ViKSeR (Ours)

A small, fluffy bird with a tired appearance perches on a metal object, possibly a bike wheel, in a sunlit spot ... The bird's feathers are glistening with sunlight, reflecting the warmth of the sun and the comfort of its resting spot ... The bird's position on the metal object provides a stable surface for it to perch on, reflecting its adaptability to urban environments. Its beak is slightly open, and its eyes closed, giving it a peaceful or sleepy demeanor.

Fig. 6: Performance of ViKSER's F-VKE module and baselines in generating captions for two images.

On the other hand, to systematically validate the effectiveness of the CoE prompting method, we conduct quantitative comparative experiments. Specifically, within the S-RR module of ViKSER, we integrate both CoE and CoT prompting strategies and evaluate their performance on the VQAv2 and A-OKVQA datasets. As shown in Table VI, ViKSER with CoE prompting consistently outperforms the CoT-based variant across all evaluation metrics. These results demonstrate that incorporating fine-grained visual knowledge as factual evidence enables CoE prompting to establish more reliable reasoning, leading to superior visual reasoning performance.

Additionally, to further demonstrate the effectiveness of the CoE prompting method, we conduct qualitative comparative experiments. Specifically, we compare the performance of ViKSER when integrated with CoE prompting versus CoT prompting on three representative visual reasoning tasks. As illustrated in Figure 7, in the first case, the CoT prompting method exhibits severe hallucination, erroneously interpreting "30" as "29", which leads to an incorrect answer. In contrast,

TABLE VI: Comparative performance between ViKSER with CoE prompting and ViKSER with CoT prompting on the VQAv2 and A-OKVQA datasets.

Methods	VQAv2				A-OKVQA	
	Ov. (%)	Y/N (%)	Num. (%)	Ot. (%)	MC. (%)	DA. (%)
ViKSER w/ CoE	88.74	98.31	75.51	86.71	92.51	88.53
ViKSER w/ CoT	71.42	76.92	61.54	69.23	79.81	75.76

the CoE prompting method successfully derives the correct response by leveraging the precise *Evidence* “thirty years of age” provided in the Evidence section, demonstrating reliable reasoning. Similarly, in the second and third cases, the CoT prompting method fails to accurately interpret visual information and again suffers from hallucination, producing incorrect answers in both instances. Notably, the CoE prompting method consistently performs well, relying on accurate *Evidence* (“make a jump” and “point to the left”) and robust reasoning to correctly solve these visual reasoning tasks. These cases demonstrate that the CoE prompting method effectively mitigates hallucination in ViKSER’s reasoning while enhancing its reliability and interpretability by incorporating fine-grained visual knowledge from the F-VKE module as factual evidence (as discussed in Section III-B).

D. Case Studies

To further validate the effectiveness of ViKSER, we conduct a qualitative analysis of its performance on two practical visual reasoning cases. As shown in Figure 8, in case (a), ViKSER identifies that the motorcyclist has a lit cigarette in his mouth while riding, by generating an image caption that contains fine-grained visual knowledge. This discovery serves as the foundation for solving the case (a). Subsequently, ViKSER utilizes the extracted visual knowledge to refine the ambiguous descriptions of the subject in the original question, resulting in a paraphrased question. Finally, through step-by-step reasoning with evidence, ViKSER infers the correct answer, “cigarette”. This practical visual reasoning case demonstrates ViKSER’s ability to extract fine-grained visual knowledge and its proficiency in utilizing visual facts as evidence for interpretable reasoning. Additionally, case (b) further demonstrates ViKSER’s self-reflection capability. Specifically, due to inevitable reasoning errors, ViKSER initially inferred an incorrect answer, “no”, in a previous reasoning process. Fortunately, with the assistance of the self-reflection mechanism, ViKSER generates a reflective message regarding its last failure, acknowledging that it had overlooked the fact that children may not pay attention to small details such as sugar on his faces while enjoying a treat. Subsequently, utilizing the reflective message, ViKSER accurately guides a new round of evidence-based reasoning and ultimately infers the correct answer, “yes”. This practical case demonstrates ViKSER’s ability to address reasoning errors through self-reflection and generate more valuable responses.

Moreover, we demonstrate the capabilities of ViKSER on more typical visual reasoning cases. The baseline models selected for comparison include LLaVa-1.5, Qwen-2.5, Blip2-

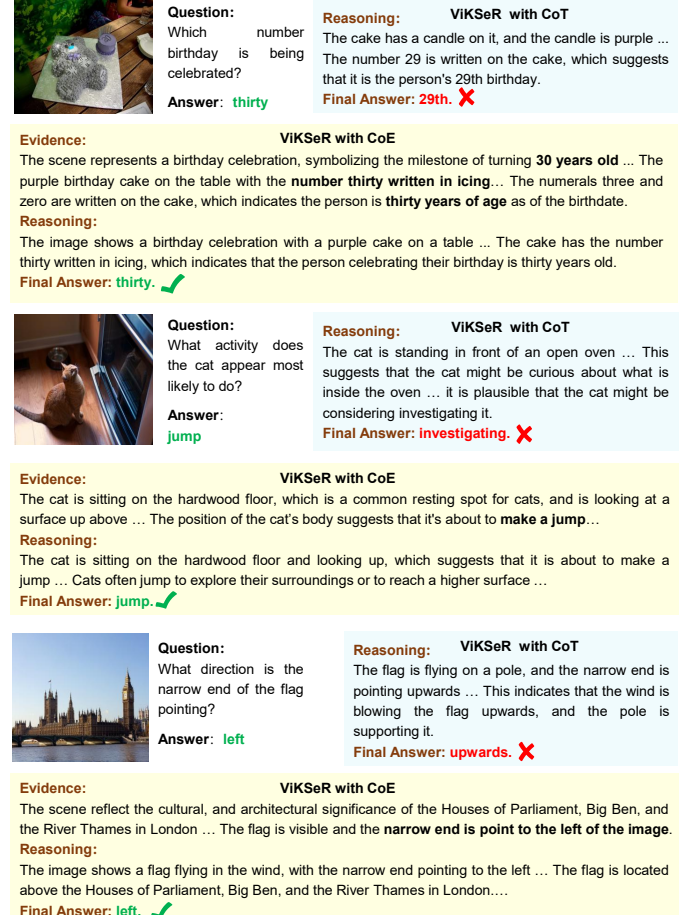


Fig. 7: Comparative performance between ViKSER with CoE prompting and ViKSER with CoT prompting on three representative visual reasoning tasks.

Flan-T5-XXL [51], and GPT-4o-mini. It is worth noting that, due to the comparatively smaller parameter scales of LLaVa-1.5, Qwen-2.5, and Blip2-Flan-T5-XXL, we implement CoT prompting to augment their reasoning abilities. In contrast, for GPT-4o-mini, which possesses a substantially larger parameter size, we directly employ it for reasoning tasks without additional prompting strategies. Detailed results are shown in Figure 9, 10, 11 and 12. Specifically, Figure 9 and 10 compare the performance of ViKSER and the baselines on two visual reasoning tasks involving short-answer questions. While all baselines fail to solve both tasks, ViKSER excels by analyzing the fine-grained visual knowledge it extracts and applying correct reasoning to answer the questions. Additionally, Figure 11 illustrates the performance of ViKSER

(a) Question: What is in his mouth ? (cigarette)

Caption: A motorcyclist wearing a helmet ... has a lit cigarette in his mouth ... smoking while riding ...

Paraphrased Question: What is in the motorcyclist's mouth while riding?

Reasoning:

1. The image shows a man wearing a helmet ... is smoking a cigarette ...
2. The presence of the lit cigarette in his mouth ...
3. Therefor, the answer to the question ... is "cigarette".

Answer: cigarette ✓

(b) Question: Will he leave the powdered sugar on his face ? (yes)

Paraphrased Question: Will the child leave the powdered sugar on his face while exploring the taste of the pastry?

Wrong Answer: no ✗

Reflection: The previous reasoning overlooked the fact that children may not pay attention to small details like the sugar on his face when enjoying a treat ...

Reasoning: The child is eating a pastry ... focusing on the food ... Given his focus on the taste of the pastry, he is likely to leave the sugar on his face ...

Answer: yes ✓

Fig. 8: The performance of ViKSER on two practical visual reasoning cases.

and the baseline models in addressing a visual reasoning task involving true/false questions. All baseline models fail to achieve satisfactory results in this task, especially Blip2-Flan-t5-xxl using CoT prompting, which fails to understand the question requirements and merely describes the image information in the answer. In contrast, ViKSER demonstrates exceptional performance, successfully solving the visual reasoning task with remarkable accuracy and proficiency. Finally, Figure 12 presents the performance of ViKSER and the baseline models in addressing a visual reasoning task involving short-answer questions. With the exception of GPT-4o-mini, all baseline models fail to achieve satisfactory results in this task. Notably, ViKSER initially produces an incorrect result during the first round of reasoning. Fortunately, leveraging the self-reflection mechanism, ViKSER identifies its mistake and re-infers the correct answer.

Question: What type of fruit is cut in half and darker than the other?

Reasoning: Llava 1.5 - CoT

The image shows a plate of food with a fork and a knife on it. The fork is silver and has a handle. The plate contains a salad with various vegetables, including tomatoes and carrots. The darker fruit is the tomato.

Final Answer: Tomato. ✗

Reasoning: Qwen2.5 - CoT

The image shows a plate of food consisting of a piece of meat, mushrooms, and a salad with various vegetables and a creamy dressing. There are no fruits visible in the image. The question asks about a fruit that is cut in half and darker than the others, it is not possible to identify any fruit based on the given image.

Final Answer: There is no fruit. ✗

Reasoning: Blip2-Flan-t5-xxl - CoT

Based on the image, we can see several fruits on the plate. Upon closer inspection, one fruit is cut in half, with its flesh clearly exposed. This cut fruit appears darker than the others, with a deep green color. Considering this color and texture, it is inferred that this fruit is a kiwi. Therefore, The fruit is a kiwi fruit.

Final Answer: kiwi. ✗

Reasoning: GPT-4o-mini

The fruit you are referring to could be an avocado. When an avocado is cut in half, the inside is typically a lighter green or yellow color, while the outer skin is darker, especially when the fruit is ripe. The flesh of the avocado is soft and creamy, with a large round pit in the center that needs to be carefully removed.

Final Answer: avocado. ✗

Caption: A appealing plate of salad features a chicken breast cut into bite-sized pieces ... The salad contains an array of cut vegetables and fruits, including grapes, lettuce and mushrooms ... adding vibrancy and freshness to the dish ... grapes are a deep purple ... A fork and knife are neatly placed beside the plate, indicating a formal dining setting.

Paraphrased Question: What type of fruit is cut in half and darker than the other fruit in the salad?

Reasoning:

The image shows a plate of food containing a salad ... The salad includes grapes, which are cut up and darker than the other fruits. The grapes are a deep purple color that is darker. The answer to the question "What type of fruit is cut in half and darker than the other fruit in the salad?" is "grapes."

Final Answer: grapes. ✓

Reasoning: ViKSeR (Ours)

A appealing plate of salad features a chicken breast cut into bite-sized pieces ... The salad contains an array of cut vegetables and fruits, including grapes, lettuce and mushrooms ... adding vibrancy and freshness to the dish ... grapes are a deep purple ... A fork and knife are neatly placed beside the plate, indicating a formal dining setting.

Paraphrased Question: What type of fruit is cut in half and darker than the other fruit in the salad?

Reasoning:

The image shows a plate of food containing a salad ... The salad includes grapes, which are cut up and darker than the other fruits. The grapes are a deep purple color that is darker. The answer to the question "What type of fruit is cut in half and darker than the other fruit in the salad?" is "grapes."

Final Answer: grapes. ✓

Fig. 9: Performance of ViKSER and baselines on a visual reasoning task involving short-answer questions.

Question: What is the white substance on top of the cupcakes?

Reasoning: Llava 1.5 - CoT

A person's hand pointing at two cupcakes with white frosting and red decorations. The frosting is white, and the decorations are red, which indicates that the cupcakes are likely vanilla flavored with strawberry toppings.

Final Answer: The white substance is frosting. ✗

Reasoning: Qwen2.5 - CoT

The image shows a close-up of a person's hand decorating cupcakes with what appears to be a white frosting or cream. The cupcakes have a light-colored base, possibly vanilla, and are topped with a dollop of white frosting, which could be buttercream or whipped cream.

Final Answer: buttercream or whipped cream. ✗

Reasoning: Blip2-Flan-t5-xxl - CoT

The image shows a cupcakes are topped with a layer of white substance. This substance has a smooth appearance, typically used to decorate cakes and enhance flavor. Based on the usage and appearance, the white substance on top of the cupcakes is frosting.

Final Answer: frosting. ✗

Reasoning: GPT-4o-mini

The white substance on top of the cupcakes appears to be frosting, likely buttercream frosting, which is commonly used for decorating cupcakes. It's creamy and can be piped into various shapes, as seen in the image. Buttercream frosting is typically made from butter, powdered sugar, and vanilla extract.

Final Answer: frosting. ✗

Caption: A hand is skillfully decorating a cupcake with frosting and a raspberry ... The frosting is the icing ... The cupcake is placed on a countertop, surrounded by baking ingredients, emphasizing the creative process in a kitchen setting ... The hand's action of pointing at the raspberry and applying the frosting highlights the attention to detail ...

Paraphrased Question: What type of fruit is cut in half and darker than the other fruit in the salad?

Reasoning:

In the image, a person's hand is skillfully decorating a cupcake with frosting and a raspberry. The frosting is the icing, which is commonly used to decorate cupcakes. Therefore, the answer to the question "What is the white frosting on the cupcakes made from?" is "icing."

Final Answer: icing. ✓

Fig. 10: Performance of ViKSER and baselines on a visual reasoning task involving short-answer questions.

Question: Is the man on the left platform going to board the train?

Reasoning: Llava 1.5 - CoT

The image shows a train on the tracks with people standing on the platform. One of the people is a man who is standing on the left platform. The train is approaching the station, and the man is likely waiting to board the train.

Final Answer: Yes. ✗

Reasoning: Qwen2.5 - CoT

The image depicts a train station with a train arriving at the platform. The person on the left platform appears to be standing near the edge, possibly waiting for the train to stop before boarding. However, there is no clear indication that this person is actively boarding the train at this moment.

Final Answer: uncertain. ✗

Reasoning: Blip2-Flan-t5-xxl - CoT

The image shows a man standing on the left platform, with a train located on the right platform. The position relationship between the train and the man is clear, standing on different platforms.

Final Answer: The man is on the left platform and the train is on the right platform. ✗

Reasoning: GPT-4o-mini

It's difficult to determine whether the man is going to board the train based on the image alone. The man's body language, position relative to the train would provide more context. If he is near the edge of the platform and facing the train, he may be preparing to board. However without additional information, it's uncertain.

Final Answer: uncertain. ✗

Caption: A blue and yellow train travels down the right side of the tracks, approaching a train station ... A man is on the other side of the tracks ... The train is carrying passengers on the platform, who are waiting to board or disembark ... The train tracks, located adjacent to the station, guide the train's movement and direction.

Paraphrased Question: Is the man on the left platform going to board the train on the right side of the tracks?

Reasoning:

The man is standing on the left platform, and the train is on the right platform. The train is moving, and the man is not boarding it. The man is far away from the other train, and he's on the other side of the tracks. The answer to the question "Is the man on the left platform going to board the train on the right side of the tracks" is "no."

Final Answer: No. ✓

Fig. 11: Performance of ViKSER and baselines on a visual reasoning task involving a true/false question.

V. LIMITATIONS

Despite the significant improvements achieved by ViKSER in visual reasoning tasks compared to existing methods, several limitations remain: 1) In *Ag-VRD*, we directly employ the CoVLM model to extract visual relationships between key entities in images. However, its simplified architecture may incompletely capture complex relational patterns, suggesting that advanced VRD methods could improve performance. 2) During the knowledge distillation process for training the causal relationship analyzer G_a and image caption generator G_c , we use ChatGPT-4o as the sole teacher model without conducting comparative experiments with other LLMs. Exploring more

 <p>Question: Why would you use this suitcase?</p> <p>Answer: luggage travel.</p>	<p>Reasoning: Llava 1.5 - CoT</p> <p>The image shows a suitcase filled with various items such as bottles, a backpack, and a teddy bear. The suitcase is open and placed on the floor. The presence of these items suggests that the suitcase is being used for transporting belongings.</p> <p>Final Answer: transporting belongings. X</p>
	<p>Reasoning: Qwen2.5 - CoT</p> <p>The image shows an open suitcase filled with various items such as toiletries, medications, and possibly some clothing, all of which appear to be personal belongings. The word "baggage" is prominently displayed, which indicates that the suitcase is used for carrying personal belongings.</p> <p>Final Answer: carrying personal belongings. ✓</p>
<p>Reasoning: Blip2-Flan-15-xxl - CoT</p> <p>The image shows an open suitcase filled with various things, including toiletries, medications, and some clothes. It is obvious that this suitcase is very large and can hold a lot of things.</p> <p>Final Answer: this suitcase can hold a lot of things. X</p>	<p>Reasoning: GPT-4o-mini</p> <p>This suitcase appears to be packed with a variety of items, suggesting it may be used for a long trip or vacation. The presence of toiletries, grooming supplies, and other personal items indicates that the owner is likely preparing for travel abroad or a family visit ... Overall, the suitcase seems suited for travel.</p> <p>Final Answer: travel. ✓</p>
	<p>Caption: ViKSeR (Ours)</p> <p>A suitcase is opened and filled with various toiletries and personal items for daily use, reflecting the process of packing for travel ... The suitcase is positioned on the floor, surrounded by other travel accessories such as a backpack ... A bag placed next to the suitcase indicates that it is being used to store or transport other items.</p> <p>Paraphrased Question: What is the purpose of this suitcase, which is filled with items necessary for daily use?</p> <p>Reasoning:</p> <p>The image shows a suitcase filled with various toiletries and personal items, indicating that it is packed for travel ... The presence of the suitcase and its contents suggest that the purpose of this suitcase is for daily use during travel.</p> <p>Incorrect Answer: daily use. X</p> <p>Self-Reflection: In the previous trial, I failed to address the question as I answer the phrase "daily use," which may not have been clear enough in context. The purpose of the suitcase is to pack for travel, so I will adjust the reasoning to focus more directly on the travel aspect.</p> <p>New Reasoning:</p> <p>The image shows an open suitcase packed with toiletries and personal items typically associated with travel ... The arrangement of items such as toiletries suggests preparation for travel ...</p> <p>Final Answer: travel. ✓</p>

Fig. 12: Performance of ViKSeR and baselines on a visual reasoning task involving short-answer questions.

powerful LLMs as alternative teacher models could potentially improve performance. 3) In Ag-SR, the self-reflection mechanism may fail to identify critical insights from prior reasoning failures during highly complex visual reasoning tasks, limiting subsequent response refinement. Mechanism optimization remains an open research direction.

VI. CONCLUSION

In this paper, we introduce ViKSeR, a new framework for visual reasoning tasks, which integrates the extraction of fine-grained visual knowledge with high interpretability and self-reinforcing reasoning capabilities. ViKSeR comprises F-VKE and S-RR modules, as well as integrates advanced mechanisms to achieve superior performance. We conduct extensive experiments on diverse public datasets. The results demonstrate that ViKSeR outperforms the latest research across public datasets, achieving new SOTA results. Our future work will focus on: 1) Exploring methods that extract finer-grained visual knowledge while performing more comprehensive visual reasoning based on overall image features. 2) Further integrating the capabilities of world models into ViKSeR.

ACKNOWLEDGMENTS

This work was supported by the National Key Research and Development Program of China (Grant No. 2022ZD0160603), and the Natural Science Foundation of Shanghai (No. 23ZR1422800).

APPENDIX

A. Training the Image Caption Generator

After obtaining the analysis reports KA'_p , the image caption generator G_c enriches the preliminary image description D

by integrating the visual knowledge from the input image I and KA'_p to generate a detailed image caption C for I . As discussed in Section III-A0b, we utilize profound-ground-truth data generated by the LLM to train the G_c . Specifically, we extract pseudo-ground-truth image caption C_p from LLM with a task-specific set of few-shot demonstrations as follows:

$$KC_p = \{C_p \mid C_p \sim P_{LLM}(I, D, A'_p)\}, \quad (6)$$

where I denotes the input image, D represents the ground-truth preliminary image description of I , and $A'_p \in KA'_p$ represents the pseudo-ground-truth analysis report. P_{LLM} denotes the LLM operating autoregressively. C_p denotes the the pseudo-ground-truth image caption sampled from P_{LLM} , and KC_p represents the set of all C_p .

Unfortunately, KC_p may contain noise and errors, adversely affecting the training of G_c . To address this, we similarly apply a post-processing mechanism to filter KA'_p into KA'_p . Specifically, for each C_p in KC_p , we use F (the pre-trained MLLM) to assess its validity score S_{C_p} based on whether C_p correctly introduces the image. If S_{C_p} exceeds the predetermined threshold τ , the corresponding C_p is retained. The process of collecting KC'_p is formalized as follows:

$$KC'_p = \{C_p \mid S_{C_p} > \tau\}, S_{C_p} = F(C_p, (I, D, A'_p)), \quad (7)$$

where C_p denotes the pseudo-ground-truth image caption. I denotes the input image, D represents the ground-truth preliminary image description. A'_p represents the pseudo-ground-truth analysis report. τ denotes the predetermined threshold. F denotes the pre-trained MLLM. With KC'_p serving as pseudo-ground-truth data, we are able to train G_c with the distillation loss L_{G_c} . The training process is formalized below:

$$L_{G_c} = - \sum_{t=1}^T \log (P_{G_c}(C'_{p,t} \mid C'_{p,t-1}, (I, D, A'_p))), \quad (8)$$

where $C'_p \in KC'_p$, $A'_p \in KA'_p$, and $T = |C'_p|$. Finally, the trained G_c and G_a collaborate to generate a detailed image caption C for the input image I .

B. Implementation Details

a) Self Reflection: As detailed in Section III-B, upon encountering an unsatisfactory result, Ag-SR engages in self-reflection through analyzing the paraphrased question, image caption, and reasoning trajectory to generate structured verbal reflection V_{ref} . Specifically, V_{ref} pinpoints erroneous reasoning steps in the previous trajectory and suggests corrective measures, enabling more accurate subsequent inferences. This iterative process continues until either (a) a satisfactory result is obtained or (b) reaching the maximum iterations. It is noteworthy that we set the maximum iteration count to 3 across all experiments.

b) Knowledge Distillation from LLM: As discussed in Section III-A0b, we utilize the knowledge reservoir embedded in LLM(e.g., ChatGPT-4o) to generate causal relationship analysis reports A'_p and detailed image captions C'_p as pseudo-ground-truth data to train causal relationship analyzer G_a and image caption generator G_c . This section details the implementation of our knowledge distillation framework. As

shown in Equation 2, given an input image I and its preliminary description D , we prompt ChatGPT-4 to analyze causal relationships between key entities' behaviors in D and their outcomes inferred from I , producing the raw output A_p . A post-processing mechanism then processes A_p to obtain the refined analysis reports A'_p (Equation 3). Subsequently, as indicated in Equation 6, we input I , D , and A'_p to ChatGPT-4, directing it to generate detailed image captions C_p that describes key entities, their behaviors, and causal inferences in natural language. Similarly, C_p undergoes the same post-processing mechanism to yield the refined image caption C'_p (Equation 7).

We distill 500 annotated pairs of A'_p and C'_p from ChatGPT-4 to serve as pseudo-ground-truth data for training. As specified in Equations 4 and 8, the implementation fine-tunes LLaVA-1.5-7B using distillation losses \mathcal{L}_{G_a} and \mathcal{L}_{G_c} over 10 epochs, yielding the G_a and G_c . The model input combines an image with a text template formed by concatenating the generation prompt with corresponding pseudo-ground-truth data. Figures 13 and 14 illustrate two examples of the text templates used for fine-tuning G_a and G_c , respectively. The complete fine-tuning procedure executes on an NVIDIA V100 server with 32GB VRAM under identical initialization conditions.

```
conversations: [{from: "human",
  value: "<image> ... # You are given an image and its
  description ... You need to find the causal relationships between
  key entities' behaviors in description and the inferred
  outcomes ... # Image Description: ..."},

{from: "gpt",
  value: "The skateboarder, using the table as an improvised
  obstacle ... is performing a trick in the air on the skateboard ...
  will to land and continue gliding ..."}]
```

Fig. 13: The example of the template used for fine-tuning G_a .

```
conversations: [{from: "human",
  value: "<image> ... # You are given a description of an
  image, including the entities in the image, their behaviors, and
  the causal relationships ... You need generate a detailed image
  caption ... Please use fluent and complete sentences ... # Image
  Description: ... Causal relationships: ..."},

{from: "gpt",
  value: "A skateboarder is mid-air, performing a dynamic trick
  above a picnic table used as an improvised obstacle, embodying
  skateboarding's inventive use of urban environments ..."}]
```

Fig. 14: The example of the template used for fine-tuning G_c .

c) Hyperparameters: As introduced in Section III-A0a, Ag-VRD utilizes a joint entity-relation validity evaluation algorithm to compute the entity-relation joint validity scores S_r^e . Our algorithm incorporates three hyperparameters: (1) γ controlling the weighting of visual relationship quantity; (2) α constraining the maximum number of relationships; and (3) θ_r^e defining the validity threshold for S_r^e to identify key relationships. To standardize the extraction of approximately four key entities per image across all experiments, we consistently set $\gamma = 0.1$, $\alpha = 4$, and $\theta_r^e = 0.55$. Additionally, when distilling pseudo-ground-truth data from the LLM to train G_a

and G_c , we introduce a hyperparameter τ in the post-processing mechanism for noise suppression. This threshold τ acts as the validity score cutoff to filter noisy data (Equations 3 and 7). Across all experiments, we set $\tau = 0.6$.

C. Generating Reasoning from PVLMs

As discussed in Section III-B, given the diversity of visual reasoning tasks, we propose a generalized, plug-and-play reasoning prompt paradigm to prompt PVLMs to activate the capacities of the S-RR module. In this section, we provide a detailed discussion of the design methodology for each prompt.

a) Specification Paraphrase: After acquiring fine-grained visual knowledge from the F-VKE module, the S-RR module prompts a PVLM to paraphrase the question text that exhibits underspecification. The prompt for specification paraphrasing is shown in Figure 15.

```
# You are an expert in question paraphrasing. Given an [Image], a
[Question] about the [Image], and an [Image Caption].
# The [Question] about the [Image] may lack sufficient
descriptions.
# Based on the [Image] and the [Image Caption], please
supplement the ambiguous descriptions in the [Question].
...
# Note: The descriptions you need to supplement in the [Question]
includes:
1. Descriptions of the main entity or subject mentioned in the
[Question].
2. Descriptions of the background of the image and main subject
that may not be mentioned in the [Question].
...
```

Fig. 15: The prompt for paraphrasing the question text with underspecification.

b) CoE Prompting: To answer the paraphrased question, the S-RR module employs CoE prompting to guide a PVLM in thinking step by step based on evidence and inferring a valuable response. As illustrated in Figure 16, CoE prompting first instructs the PVLM to leverage the visual information in the image and its caption to address the input question. Subsequently, the PVLM is encouraged to think step-by-step with evidence and generate both the answer and the step-by-step reasoning based on evidence. This reasoning framework helps the PVLM focus on the relevant visual information in the image and caption, using it as evidence to support interpretable reasoning.

```
# You are an expert in Visual Reasoning.
# Given an [Image], and a useful [Caption] about the [Image], as
well as a [Question] about the [Image] to answer.
...
# Your task is to analyze the [Question], [Image] and [Caption] to
construct a reasonable reasoning path to provide an Answer to
the [Question].
...
# Think step by step with evidence.
# Generate both [Answer] and [Step-by-step-reasoning-with-
evidence].
...
```

Fig. 16: The prompt for the CoE prompting technique.

c) *Self Reflection*: With the aim of addressing low-quality responses, the S-RR module prompts a PVLM to self-reflect on past failures and seek more valuable responses. As illustrated in Figure 17, the PVLM is tasked with analyzing the reasoning trajectory of past failures, reflecting on their causes, and formulating a high-level plan to prevent similar failures in the future. Finally, the PVLM will derive a more valuable answer based on the reflection information and the high-level plan.

```
# You are an advanced reasoning agent capable of improving
based on self-reflection.

# You will be given the Result and [Trajectory] of a previous
reasoning trial, where you were asked to answer a [Question] but
were unsuccessful in doing so.

...
# Based on the given [Image], [Question], and the [Trajectory] of
the previous round of VQA reasoning, diagnose the possible
reason for failure or phrasing discrepancy in a few sentences, and
devise a new, high-level plan to mitigate similar failures. Please use
complete sentences.

# Finally you should provide your Answer to the [Question] based
on your Reflection.
```

Fig. 17: The prompt for the self-reflection mechanism.

REFERENCES

- [1] A. Steiner, A. S. Pinto, M. Tschannen, D. Keysers, X. Wang, Y. Bitton, A. Gritsenko, M. Minderer, A. Sherbondy, S. Long *et al.*, “Paligemma 2: A family of versatile vlms for transfer,” *arXiv preprint arXiv:2412.03555*, 2024.
- [2] H. Liu, C. Li, Q. Wu, and Y. J. Lee, “Visual instruction tuning,” 2023.
- [3] A. Kamath, M. Singh, Y. LeCun, G. Synnaeve, I. Misra, and N. Carion, “Mdetr-modulated detection for end-to-end multi-modal understanding,” in *Proceedings of the IEEE/CVF international conference on computer vision*, 2021, pp. 1780–1790.
- [4] J. Wu, X. Hu, Y. Wang, B. Pang, and R. Soricut, “Omni-smola: Boosting generalist multimodal models with soft mixture of low-rank experts,” in *Proceedings of the IEEE/CVF Conference on Computer Vision and Pattern Recognition*, 2024, pp. 14 205–14 215.
- [5] A. Ray, F. Radenovic, A. Dubey, B. Plummer, R. Krishna, and K. Saenko, “Cola: A benchmark for compositional text-to-image retrieval,” *Advances in Neural Information Processing Systems*, vol. 36, 2024.
- [6] T. Gupta and A. Kembhavi, “Visual programming: Compositional visual reasoning without training,” in *Proceedings of the IEEE/CVF Conference on Computer Vision and Pattern Recognition (CVPR)*, June 2023, pp. 14 953–14 962.
- [7] F. He, Y. Wang, X. Miao, and X. Sun, “Interpretable visual reasoning: A survey,” *Image and Vision Computing*, vol. 112, p. 104194, 2021.
- [8] K.-P. Chang, C.-P. Huang, W.-Y. Cheng, F.-E. Yang, C.-Y. Wang, Y.-H. Lai, and Y.-C. F. Wang, “Rapper: Reinforced rationale-prompted paradigm for natural language explanation in visual question answering,” in *Proceedings of the 2024 International Conference on Learning Representations (ICLR)*. OpenReview, 2024. [Online]. Available: <https://openreview.net/forum?id=bshfchPM9H>
- [9] A. Prasad, E. Stengel-Eskin, and M. Bansal, “Rephrase, augment, reason: Visual grounding of questions for vision-language models,” in *The Twelfth International Conference on Learning Representations*, 2024. [Online]. Available: <https://openreview.net/forum?id=L4nOxziGf9>
- [10] Y. Zhang, S. Chen, and Q. Zhao, “Toward multi-granularity decision-making: Explicit visual reasoning with hierarchical knowledge,” in *Proceedings of the IEEE/CVF International Conference on Computer Vision*, 2023, pp. 2573–2583.
- [11] M. Deitke, C. Clark, S. Lee, R. Tripathi, Y. Yang, J. S. Park, M. Salehi, N. Muennighoff, K. Lo, L. Soldaini *et al.*, “Molmo and pixmo: Open weights and open data for state-of-the-art multimodal models,” *arXiv preprint arXiv:2409.17146*, 2024.
- [12] Y. Bazi, M. M. A. Rahhal, L. Bashmal, and M. Zuair, “Vision–language model for visual question answering in medical imagery,” *Bioengineering*, vol. 10, no. 3, p. 380, 2023.
- [13] A.-M. Marcu, L. Chen, J. Hünermann, A. Karnsund, B. Hanotte, P. Chidananda, S. Nair, V. Badrinarayanan, A. Kendall, J. Shotton *et al.*, “Lingoqa: Visual question answering for autonomous driving,” in *European Conference on Computer Vision*. Springer, 2024, pp. 252–269.
- [14] R. Y. Zakari, J. W. Owusu, H. Wang, K. Qin, Z. K. Lawal, and Y. Dong, “Vqq and visual reasoning: An overview of recent datasets, methods and challenges,” *arXiv preprint arXiv:2212.13296*, 2022.
- [15] S. Pezzelle, “Dealing with semantic underspecification in multimodal nlp,” *arXiv preprint arXiv:2306.05240*, 2023.
- [16] H. Cui, X. Fang, Z. Zhang, R. Xu, X. Kan, X. Liu, Y. Yu, M. Li, Y. Song, and C. Yang, “Open visual knowledge extraction via relation-oriented multimodality model prompting,” *Advances in Neural Information Processing Systems*, vol. 36, 2024.
- [17] C. Yang, R. Xu, Y. Guo, P. Huang, Y. Chen, W. Ding, Z. Wang, and H. Zhou, “Improving vision-and-language reasoning via spatial relations modeling,” in *Proceedings of the IEEE/CVF Winter Conference on Applications of Computer Vision (WACV)*, January 2024, pp. 769–778.
- [18] H. Cui, R. Lin, N. Zalmout, C. Zhang, J. Shang, C. Yang, and X. Li, “Pv2tea: Patching visual modality to textual-established information extraction,” *arXiv preprint arXiv:2306.01016*, 2023.
- [19] W. Jiang, L. Ma, Y.-G. Jiang, W. Liu, and T. Zhang, “Recurrent fusion network for image captioning,” in *Proceedings of the European Conference on Computer Vision (ECCV)*, September 2018.
- [20] T. Yao, Y. Pan, Y. Li, Z. Qiu, and T. Mei, “Boosting image captioning with attributes,” in *Proceedings of the IEEE International Conference on Computer Vision (ICCV)*, Oct 2017.
- [21] Y. Hu, H. Hua, Z. Yang, W. Shi, N. A. Smith, and J. Luo, “Promptcap: Prompt-guided image captioning for vqa with gpt-3,” in *Proceedings of the IEEE/CVF International Conference on Computer Vision (ICCV)*, October 2023, pp. 2963–2975.
- [22] Z. Fang, J. Wang, X. Hu, L. Liang, Z. Gan, L. Wang, Y. Yang, and Z. Liu, “Injecting semantic concepts into end-to-end image captioning,” in *Proceedings of the IEEE/CVF Conference on Computer Vision and Pattern Recognition (CVPR)*, June 2022, pp. 18 009–18 019.
- [23] Z. Li, X. Zhu, X. Zhang, Z. Zhang, and Z. Lei, “Visual commonsense based heterogeneous graph contrastive learning,” *arXiv preprint arXiv:2311.06553*, 2023.
- [24] J. Li, D. Chen, Y. Hong, Z. Chen, P. Chen, Y. Shen, and C. Gan, “Covlm: Composing visual entities and relationships in large language models via communicative decoding,” in *The Twelfth International Conference on Learning Representations, ICLR 2024, Vienna, Austria, May 7-11, 2024*. OpenReview.net, 2024. [Online]. Available: <https://openreview.net/forum?id=PHGxChm115>
- [25] A. Zareian, S. Karaman, and S.-F. Chang, “Bridging knowledge graphs to generate scene graphs,” in *Computer Vision – ECCV 2020*, A. Vedaldi, H. Bischof, T. Brox, and J.-M. Frahm, Eds. Cham: Springer International Publishing, 2020, pp. 606–623.
- [26] H. Lang, M. N. Agrawal, Y. Kim, and D. Sontag, “Co-training improves prompt-based learning for large language models,” in *International Conference on Machine Learning*. PMLR, 2022, pp. 11 985–12 003.
- [27] Y. Yu, Y. Zhuang, J. Zhang, Y. Meng, A. J. Ratner, R. Krishna, J. Shen, and C. Zhang, “Large language model as attributed training data generator: A tale of diversity and bias,” *Advances in Neural Information Processing Systems*, vol. 36, 2024.
- [28] T. Kojima, S. S. Gu, M. Reid, Y. Matsuo, and Y. Iwasawa, “Large language models are zero-shot reasoners,” *Advances in neural information processing systems*, vol. 35, pp. 22 199–22 213, 2022.
- [29] X. Chen, X. Wang, S. Changpinyo, A. Piergiovanni, P. Padlewski, D. Salz, S. Goodman, A. Grycner, B. Mustafa, L. Beyer *et al.*, “Pali: A jointly-scaled multilingual language-image model,” *arXiv preprint arXiv:2209.06794*, 2022.
- [30] M. Kayser, O.-M. Camburu, L. Salewski, C. Emde, V. Do, Z. Akata, and T. Lukasiewicz, “e-vil: A dataset and benchmark for natural language explanations in vision-language tasks,” in *Proceedings of the IEEE/CVF international conference on computer vision*, 2021, pp. 1244–1254.
- [31] F. Sammani, T. Mukherjee, and N. Deligiannis, “NLx-gpt: A model for natural language explanations in vision and vision-language tasks,” *CoRR*, vol. abs/2203.05081, 2022. [Online]. Available: <https://doi.org/10.48550/arXiv.2203.05081>
- [32] C. Yang, R. Xu, Y. Guo, P. Huang, Y. Chen, W. Ding, Z. Wang, and H. Zhou, “Improving vision-and-language reasoning via spatial relations modeling,” in *Proceedings of the IEEE/CVF Winter Conference on Applications of Computer Vision (WACV)*, January 2024, pp. 769–778.
- [33] J. Achiam, S. Adler, S. Agarwal, L. Ahmad, I. Akkaya, F. L. Aleman, D. Almeida, J. Altenschmidt, S. Altman, S. Anadkat *et al.*, “Gpt-4 technical report,” *arXiv preprint arXiv:2303.08774*, 2023.

- [34] J. Wei, X. Wang, D. Schuurmans, M. Bosma, brian ichter, F. Xia, E. H. Chi, Q. V. Le, and D. Zhou, “Chain of thought prompting elicits reasoning in large language models,” in *Advances in Neural Information Processing Systems*, A. H. Oh, A. Agarwal, D. Belgrave, and K. Cho, Eds., 2022. [Online]. Available: https://openreview.net/forum?id=_VjQIMeSB_J
- [35] N. Shinn, F. Cassano, A. Gopinath, K. Narasimhan, and S. Yao, “Reflexion: Language agents with verbal reinforcement learning,” *Advances in Neural Information Processing Systems*, vol. 36, 2024.
- [36] Y. Goyal, T. Khot, D. Summers-Stay, D. Batra, and D. Parikh, “Making the v in vqa matter: Elevating the role of image understanding in visual question answering,” in *Proceedings of the IEEE conference on computer vision and pattern recognition*, 2017, pp. 6904–6913.
- [37] D. Schwenk, A. Khandelwal, C. Clark, K. Marino, and R. Mottaghi, “A-okvqa: A benchmark for visual question answering using world knowledge,” in *European conference on computer vision*. Springer, 2022, pp. 146–162.
- [38] D. Gurari, Q. Li, A. J. Stangl, A. Guo, C. Lin, K. Grauman, J. Luo, and J. P. Bigham, “Vizwiz grand challenge: Answering visual questions from blind people,” in *Proceedings of the IEEE Conference on Computer Vision and Pattern Recognition (CVPR)*, June 2018.
- [39] Z. Ma, J. Hong, M. O. Gul, M. Gandhi, I. Gao, and R. Krishna, “@ crepe: Can vision-language foundation models reason compositionally?” in *Proceedings of the 2023 IEEE/CVF Conference on Computer Vision and Pattern Recognition*. IEEE, 2023, pp. 10910–10921. [Online]. Available: <https://doi.org/10.1109/CVPR52729.2023.01050>
- [40] Q. Team, “Qwen2.5-vl,” January 2025. [Online]. Available: <https://qwenlm.github.io/blog/qwen2.5-vl/>
- [41] G. OpenAI, “4o mini: Advancing cost-efficient intelligence, 2024,” URL: <https://openai.com/index/gpt-4o-mini-advancing-cost-efficient-intelligence>, 2024.
- [42] OpenAI, “Hello gpt-4o,” <https://openai.com/index/hello-gpt-4o/>, 2024, accessed 15 March 2025.
- [43] ——, “Introducing gpt-5,” <https://openai.com/zh-Hans-CN/index/introducing-gpt-5/>, 2025, published on 2025-08-09. Accessed: 2025-08-22.
- [44] K. Ranasinghe, S. N. Shukla, O. Poursaeed, M. S. Ryoo, and T.-Y. Lin, “Learning to localize objects improves spatial reasoning in visual-llms,” in *Proceedings of the IEEE/CVF Conference on Computer Vision and Pattern Recognition*, 2024, pp. 12977–12987.
- [45] X. Zhang, D. Li, B. Liu, Z. Bao, Y. Zhou, B. Yang, Z. Liu, Y. Zhong, Z. Zhao, and T. Yuan, “Himix: Reducing computational complexity in large vision-language models,” *arXiv preprint arXiv:2501.10318*, 2025.
- [46] Y. Liu, G. Bai, L. Chenji, S. Li, Z. Zhang, R. Liu, and W. Guo, “Eliminating the language bias for visual question answering with fine-grained causal intervention,” in *2024 IEEE International Conference on Multimedia and Expo (ICME)*. IEEE, 2024, pp. 1–6.
- [47] Z. Hu, P. Yang, B. Li, and Z. Wang, “Multi-agents based on large language models for knowledge-based visual question answering,” *arXiv preprint arXiv:2412.18351*, 2024.
- [48] M. Li, H. Li, Z. Du, and B. Li, “Diversify, rationalize, and combine: Ensembling multiple qa strategies for zero-shot knowledge-based vqa,” *arXiv preprint arXiv:2406.12746*, 2024.
- [49] B. Plüster, J. Ambsdorf, L. Braach, J. H. Lee, and S. Wermter, “Harnessing the power of multi-task pretraining for ground-truth level natural language explanations,” *CoRR*, vol. abs/2212.04231, 2022. [Online]. Available: <https://doi.org/10.48550/arXiv.2212.04231>
- [50] H. Singh, P. Zhang, Q. Wang, M. Wang, W. Xiong, J. Du, and Y. Chen, “Coarse-to-fine contrastive learning in image-text-graph space for improved vision-language compositionality,” *arXiv preprint arXiv:2305.13812*, 2023.
- [51] J. Li, D. Li, S. Savarese, and S. Hoi, “Blip-2: Bootstrapping language-image pre-training with frozen image encoders and large language models,” in *International conference on machine learning*. PMLR, 2023, pp. 19730–19742.